the original orientation of the aragonite plates, which was with the [001] axis perpendicular to the surface. The crystal was then tilted to the <102> to confirm the structure. The regions marked as corresponding to calcite. The region B which is the transition layer is characterized by larger crystals and probably corresponds to a mix of the $CaCO_3$ phases. The structure and growth mechanism of the mollusc shells has been extensively studied (11-15). Schaffer et. al. (15) have suggested a growth mechanism for the aragonite plates. Those authors suggest that the pores on the material allow the plates from one layer to the next without interruption. This mechanism will ensure the perfect alignment of the plates. We have confirmed the presence of pores on the plate surface. This is shown in Fig. 10. The very strong dark contrast on the pores clearly shows that they are not surface pores, but that they run deep into the crystallites. It also should be noted that in many cases no grain boundaries are formed between crystallites. This seems to confirm the growth mechanism proposed by Schaffer et. al. (15). However in this work we have found a new phenomenae not reported before, the transition layer between the calcite and the aragonite plates. Near to the molusc the material formed corrésponds to calcite A major distance from the molusc, it corresponds to aragonite. It has been suggested by Falini et. al. (16) that this phenomenae is due to the organic material layer that acts as a template for the growth of the crystallites. This material is a layer of β-chitin which is sandwiched between two layers of glycine and alanine rich proteins. Those authors show that they can induce either aragonite and calcite by using different combinations of macromolecules.

A final point to address is how the final gyroid shape of the shell is achieved from flat rectangular plates. The mechanism is shown in figure 11 a) and b). A step structure is formed between arrays of plates as shown in the figure. Similar to a stepped single crystal, the presence of an array of steps induces the curvature. However the surfaces of the plates also show facceting at the microscopic level: The gyroid structure is then due to steps at two different level of hierarquical organization.

The resultant shell is therefore a prime example of a material with elasticity, high resistance to fracture and low weight structure.

Conclusion.

We have shown that nanoporous silica can be formed in many different shapes that mimic the shell formation. We have shown the structure of some natural materials. By learning the ways in which living organisms have developed materials and synthesis of similar materials. We will be able to develop new materials with improved performance.

Acknowledgements: This project was supported by CONACYT through the grant Coloides Cuánticos, Puntos Cuánticos y Nanoparticulas.

References

1. C.T. Kresge, M.E. Lenowicz, W.J. Roth, J.C. Vartuli, J.C. Beckk. *Nature* 359, 710 (1992).
2. J.C. Beck, J.C. Vartuli, W.J. Roth, M.E. Lenowicz, C.T. Kresge, K.D. Schmidtt, W. Chu, D.H. Olson, E.W. Shepard, S.B. Cullen, J.B. Higgins and Schlenker. *J. am Chem. Soc.* 114, 10834, (1992)
3. H. Yang, A. Kuperman, S. Mamiche-Afara and G. Ozin. *Nature* 703, (1996).
4. M. Trau, N. Yao, E. Kim, Y. Xia, G.M. Whitesides and I.A. Aksay. *Nature*, 390, 674 (1997).
5. D.W. Thompson, On-Grouth and Form. Cambridge University Press (1942).
6. S. Mann and G.A. Ozin. *Nature* 382, 313 (1996).
7. G. Ozin, H. Yang, I. Sokolov and N. Coombs. *Advanced Materials*. 9, 662, (1997).
8. H. Yang, N. Coombs and G.A. Ozin. *Nature*. 386, 692 (1997).
9. D. Williams and B. Carter. Transmission Electron Microscopy.
10. J.M. Garcia Ruiz. *J. Of Cryst. Grouth*. 73, 251 (1985).
11. L. Addadi and S. Weiner. *Nature* 389, 912 (1997).
12. N.J. Watanabe. *Ultrastructural Research* 12, 351 (1965)
13. S. Weiner and W. Traub. *Phil. Trans. R. Soc. Lond.* B304, 425 (1984).
14. V. Watanabe and K. Wilbur. *Nature* 188, 334 (1960).
15. T. Schaffer, C. Ionescu, R. Proksch, M. Fritz, D. Walters, N. Almquist, C. Zaremba, A. Belcher, B.L. Smith, G. Stucky, D. Morse and P. Hansma. *Chem. Mat.* 9, 1731, (1997).
16. G. Falini, S. Albeck, S. Weiner and L. Addadi. *Science* 271, 67 (1996).

Synthesis, Fundamental Properties and Applications of Nanocrystals, Sheets, Nanotubes and Cylinders Based on Layered Transition Metal Chalcogenides

R. R. Chianelli, Gilles Berhault
Chemistry Dept. of University, at El Paso Texas, USA &
P. Santiago, D. Mendoza, A. Espinosa, J. A. Ascencio and M. José Yacamán
Instituto Nacional de Investigaciones Nucleares, México

Folded and disordered MoS_2 and other transition metal chalcogenides such as WS_2 and ReS_2 have two-dimensional layered structures. A consequence of this two-dimensional macromolecular nature is the existence of highly folded and disordered structures. These structures have been

Address for Correspondence :R. R. Chianelli ,Chemistry Department University Texas El Paso, 79968-0513P, USA. Tel : +1 915 747 7555, Fax : +1 (15 747 5748, Email : rchianelli@utep.edu.

recognized for a long time as "rag" and "tubular" structures and are useful as catalytic materials. More recently, formation of nanotubes and nested nanotubes of WS_2 and MoS_2 have been reported and described as large fullerene-like structures. The ability of MoS_2 and related compounds to form these structures remains unclear and is the subject of intense study. The study of these materials has been hindered by the inability to synthesize them in large quantities. This situation is similar to early days of research in fullerenes that progressed slowly until improved synthetic methods led to larger quantities being available. The purpose of this report is to review the synthesis of "rag" and "tubular" MoS_2 and related materials and to discuss recent results.

Introduction

In recent years the discovery of carbon nanotubes by Ijima triggered a very important new area of materials science[1]. Indeed the many interesting properties of carbon nanotubes make them very promising materials for various applications[2]. For example, theory predicted that carbon nanotubes have high mechanical strength and stiffness[3,4]. These theoretical predictions have found experimental confirmation[5]. Also, the possibility of using nanotubes for nanolithography has been demonstrated.[6]

Nanoparticles based on layered transition metal chalcogenides (LTMC's) have been important in the fields of catalysis and lubrication. However, it has been only recently recognized that these materials appear in many highly folded and disordered structures described as: cylinders, nested cylinders, nanotubes, single sheets, folded sheets, and nanocrystals. Reports of these structures and synthetic approaches to them now regularly appear in the literature, but relatively little has been reported on their fundamental properties and the chemical origins of the structures. This is in contrast to the rapidly expanding literature on similar carbon nanostructures described above. The highly bent and folded LTMC structure may be considered analogous to the carbon nanostructures with similar but as yet unrealized potential in many new applications.

The LTMCs have found a remarkably diverse set of applications. MoS_2 and WS_2 catalysts have been used for the removal of sulfur and nitrogen from petroleum feedstocks for over 50 years[7,8]. MoS_2 is also used as a lubricant additive[9]. TiS_2 and MoS_2 can act as cathodes in lithium nonaqueous batteries[10,11] and have interesting and useful intercalation chemistry[12]. WS_2, WSe_2, TiS_2, MoS_2, $MoSe_2$, and $MoTe_2$ are all semiconductors with unusual properties and potential electronic applications[13].

Most of these unusual and useful properties arise from the highly anisotropic physical properties that are due to weak bonding between layers; where a layer consists of a monolayer of metal atoms clad by covalently bonded chalcogen atoms. For example, weak bonding between layers leads to the useful lubrication properties. Weak bonding between layers also leads to nearly two-dimensional confinement of optically excited electrons and holes which in turn leads to excitonic optical absorption peaks which can be observed at room temperature. The variety of transition metals (Ti, V, Cr, Zr, Nb, Mo, Hf, Ta, W) which exist in layered structures coupled with the choice of chalcogen (S, Se, Te) leads to a rich variability in their physics and chemistry. This variability in properties results in a family of compounds with wide array of useful applications.

Synthesis of Layered Transition Metal Chalcogenides

LTMC's with different nanoscale structures have been synthesized recently by a variety of approaches. Tenne and collaborators reported the gas-phase synthesis of fullerene-like structures of WS_2[14] and of cylinders and nested cylinders of MoS_2[15]. Persans and collaborators[16,17] and Chianelli et al.,[18,19] have reported on the preparation and optical characterization of crystalline nanoparticles prepared by intercalation and ultrasonic fragmentation of bulk crystals. Frindt, Morrison and collaborators have reported the synthesis and preliminary characterization of composites based on single sheets of MoS_2 [20,21,22]. Wilcoxon and collaborators have reported the growth of MoS_2 nanoparticles using micelle techniques[23,24,25]. These structures are related to one another and to the well known "poorly crystalline" and "rag like" layered transition metal sulfides[26,27,28].

Recently, synthesis of these materials has focused on high temperature methods which occur above 650°C. These methods involve such techniques as growth from the gas phase in which MoO_3 in the vapor phase is reacted with H_2S in a carrier gas producing nested cylinders and nanotubes, designated by the authors as inorganic fullerenes[29]. These methods suffer from the difficulty of producing large amounts of materials.

A general method for preparing the transition metal dichalcogenides at or near ambient temperatures was reported by Chianelli[30]. The materials thus produced have physical properties significantly different from those produced at higher temperatures. By appropriate adjustment of parameters, poorly crystalline or amorphous powders, gels, glasses, or homogeneous dispersions of chalcogenides can be prepared. Additionally, normally crystalline compounds can be prepared, and because the preparations take place below 400°C, portions of the transition metal-sulfur phase diagrams not previously studied are now accessible. Often the materials prepared by this method contain examples of the highly folded and disordered materials described previously. An example of typical low temperature

metathetical reaction in solution is:

$$TX_4 + 2A_2Y \rightarrow TY_2 + 4AX \quad (1)$$

where T = transition metal; X = salt anion (Cl-, carboxylate, etc.); A = alkali-like cation (Li+, Na+, NH_4+, etc.); and Y = chalcogenide anion. Since both the transition-metal ions and chalcogenides are capable of existing in several oxidation states, redox reactions such as Eq. (2) are also be possible:

$$TX_5 + 5/2A_2Y \rightarrow TY_2 + 5AX + 1/2Y \quad (2)$$

The high stability of the oxides and hydroxides of the early transition metals rules out aqueous environments for all such reactions; in fact, hydroxylic solvents in general (alcohols and carboxylic acids) are too reactive to serve as solvents for TX_4 or TX_5. Furthermore, hydrogen sulfide is not a viable source of chalcogenide ion at ambient temperature, since only traces of product form with $TiCl_4$.

The variability of the technique is illustrated considering the synthesis of TiS_2 but it is easily applicable to any other transition metal sulfide. Even in the absence of oxygen from air or water, the reaction of $TiCl_4$ with H_2S has an unfavorable equilibrium direction at temperatures less than about 400°C. By using a more reactive (ionic) source for the chalcogenide (or equivalently by 'activating' hydrogen sulfide by the addition of ammonia or amines) the reaction to form the transition-metal chalcogenides proceeds readily and quantitatively at ambient temperatures. Lithium sulfide was found to be the most convenient source of sulfide ion:

$$TiCl_4 + 2Li_2S \rightarrow TiS_2 + 4LiCl \quad (3)$$

Convenient solvents for ambient-temperature precipitation are tetrahydrofuran (THF) or ethyl acetate (EA). Both give dark precipitates, which are easily filtered. The TiS_2 produced is amorphous to X-rays but in other aspects such as reaction with n-butyl lithium behaved as normal crystalline TiS_2. Repeated washings with the solvent completely remove the LiCl. Crystalline TiS_2 powders can be produced by heating amorphous TiS_2 at 400-600°C in sealed quartz tubes with careful exclusion of oxygen. Crystalline TiS_2 can also be produced in the ambient-temperature range as the amorphous TiS_2 by letting the reaction proceed much more slowly. This result indicates that the amorphous TiS_2 is either a unique phase or consists of randomly folded sheets of TiS_2, which have not been allowed to crystallize by the rapidity of precipitation.

During the study of non-aqueous precipitation it was discovered that under various conditions gels could be produced. These gels, if pumped under vacuum and heated to greater than 300°C, yielded a black, glassy solid having an amorphous X-ray powder diffraction pattern. Scanning electron microscopy (SEM) revealed conchoidal fractures:

$$TiCl_4 + 4NR_3 + 2H_2S \rightarrow TiS_2(gel) + 4R_3NH_4Cl \quad R = hexyl \quad (4)$$

The gel does not form when NH_3 is used instead of the long-chain amine suggesting that the size of the R group is critical to gel formation. This suggests that the long-chain amines are complexed to the newly formed TiS, stabilizing gel formation.

Under a wide variety of conditions the precipitated solid remained completely or partially dispersed. For example, when a yellowish solution of $TiCl_4$ in PC (propylene carbonate) was added to a white slurry of Li_2S in PC, the solution immediately turned intensely black. No solids could be filtered out and this black liquid remained stable for several years. Since it was established in several ways that the reaction of $TiCl_4$ with Li_2S is a straight forward one yielding TiS_2 + LiCl, the black liquid was likely a colloidal dispersion of TiS_2 in the dense liquid PC. Evidence points to a colloidal dispersion of the sulfur-metal-sulfur layers. LiCl can be removed by repeated flocculation of the dispersed TiS_2 with a non-dispersing solvent such as ethyl acetate, pouring off the liquid and then re-dispersing with PC.

Poorly crystalline dichalcogenides are prepared by heating in a sulfiding atmosphere the amorphous dichalcogenides prepared by the methods described above. This heating causes the dichalcogenides to crystallize partially in a structure called the 'rag' structure. For example, a highly disordered material was prepared by heating several grams of amorphous MoS_2 for 2 h at 400°C in a stream of H_2 mixed with 15% H_2S. The rag consists of several stacked but highly folded and disordered MoS_2 layers. Although only 2 to 3 nm thick in the stack direction, the layers extend several thousand angstroms perpendicular to the stack direction. By varying the conditions of preparation, one can vary the number of stacks and the dimensions of the layers. The existence of the rag structure further demonstrates the flexibility and macromolecular nature of the dichalcogenide layers. Many of these samples contained tube like structures, which we believe to be nanotubes.

WS_2, ReS_2, and OsS_2 can also be prepared in the poorly crystalline form by heating the amorphous sulfides in a H_2/H_2S atmosphere at 400°C. ReS_2 exhibited particularly disordered structure and may be the most

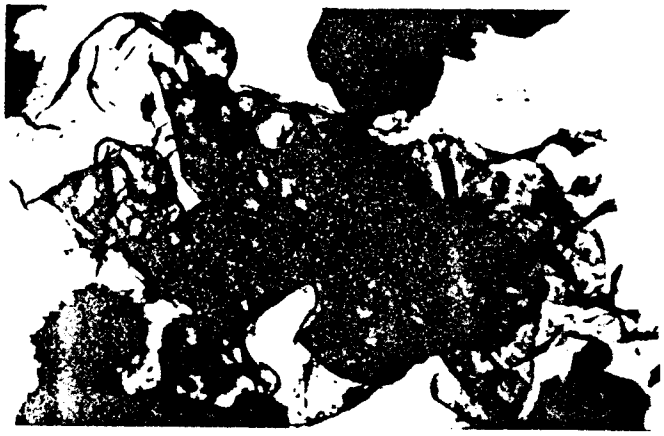

Molybdenum in the "Rag Structure"

Figure 1. MoS_2 in the "rag structure" from: R.R. Chianelli, E. Prestridge, T. Pecoraro, and J.P. DeNeufville, Science 203 (1979) 1105.

promising material for production of large amounts of nanotubes and fullerene like materials. Further developments made in preparing transition metal dichalcogenides at low temperature have been reviewed by Schleich. The use of tetraalkylammonium thiomolybdates yielded extremely disordered materials that incorporated carbon. It is believed that this impurity increases the ability of the MoS_2 to fold and form disordered materials. Ultrasonic treatment of crystalline MoS_2 is another low temperature method, which may be used to produce highly folded and disordered materials from pure starting materials[18].

Folding in the Layered Transition Metal Chalcogenides

A consequence of the two dimensional macromolecular nature of MoS_2 (and other layered transition metal chalcogenides such as WS_2 and ReS_2) is the existence of highly folded and disordered structures. These structures have been recognized for a long time. "Rag" and "tubular" structures were first reported by Chianelli et al.,[32] and studied for their usefulness as catalytic materials.

Figure 1 shows folded and disordered sheets of MoS_2. Rolled sheets of MoS_2 can also be seen which at lower magnification give the appearance of "crystalline needles". Interest in these structures has been renewed with the development and importance of carbon nanotubes and the discovery of large inorganic nanotube structures[33]. Figure 2 shows some of the many structures that have been prepared using high temperature methods and which are currently under study for potential application.

Recently transition metal trichalcogenides have been synthesized at high temperatures in a variety of shapes. The trichalcogenides such as $NbSe_3$, TiS_3 and others have layered as well as chain like structures[34]. These objects exhibit unusual morphologies at larger than atomic scales as shown in Figure 3. Morphologies observed include

Tungsten Disulfide "Tubes"

R. Tenne et al., Nature, 360(1992)444

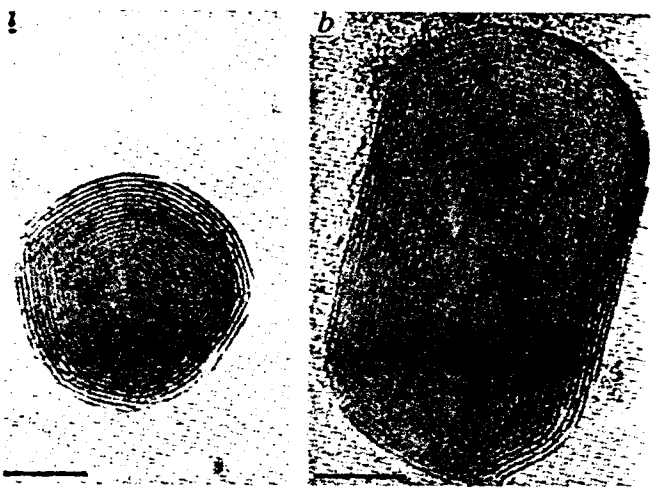

Tungsten Disulfide

Figure 2. WS_2 nanotubes from: R. Tenne et al, *Nature*, 360, 444(1992).

"wheels", "tubes", "rods" and numerous other shapes.

The ability to synthesize shapes such as these from materials that can be metals, magnets, semiconductors and insulators have led to speculation regarding the construction of micro-machines. For example, the "wheel" shown in Figure 3 if magnetic, might be incorporated into a micro-electric motor. As another example, a micro-battery might be constructed based on the intercalating abilities of the LTMCs. Fabrication seems feasible although reproducible synthesis in large uniform quantities remains a problem and possibilities for micro-machine devices seem extensive.

Nature of Folding in Layered Transition Metal Chalcogenides

Folded and disordered MoS_2 structures may be analogous in nature to large fullerene structures. The cause of the ability of MoS_2 and related compounds to form these structures remains unclear and is the subject of study. The study of these materials has been hindered by

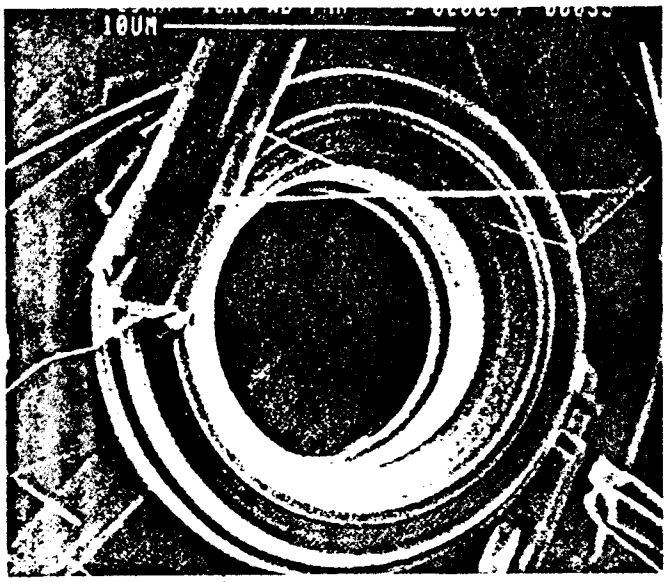

Figure 3. $NbSe_3$ "wheels" from: F.A. Trumbore and L.W. ter Haar, *Chemistry of Materials*, 1989, 1, 490.

the inability to synthesize large quantities of the material. This situation is similar to early days of research in carbon fullerenes and nanotubes that progressed slowly until improved synthetic methods led to larger quantities being available. Speculation on the cause of folding and curvature in these materials falls into three categories:

1. The ability of stoichiometric LTMC layers and chains to "bend:" This is clearly the case in materials such as TiS_2 that are observed to fold and bend during intercalation reactions. The dynamic bending and folding which occurs during these reactions is also seen to "anneal" after the reaction returning the material to an ordered crystalline state.
2. The existence of alternate coordination and therefore stoichiometry in analogy to carbon based fullerenes.
3. Stoichiometric variation within the material allowing building of closed rings, etc.: This maybe the case in more complex LTMCs such as Cylindrite ($FePb_3Sn_4Sb_2S_{14}$).[35]

In the remainder of this report we concentrate on the first category. There is at this writing no evidence reported suggesting that alternate coordination is possible. Stoichiometric variation is possible but complex. TiS_2 and MoS_2 are the best examples of nanotube formation and of bending and folding in the LTMC family. Nanotubes have been observed in MoS_2 mineral samples and TiS_2 exhibits flexible folding and bending as described above. Nanotubes have not yet been observed in TiS_2 but may be expected in analogy to MoS_2, because of their similar structures.

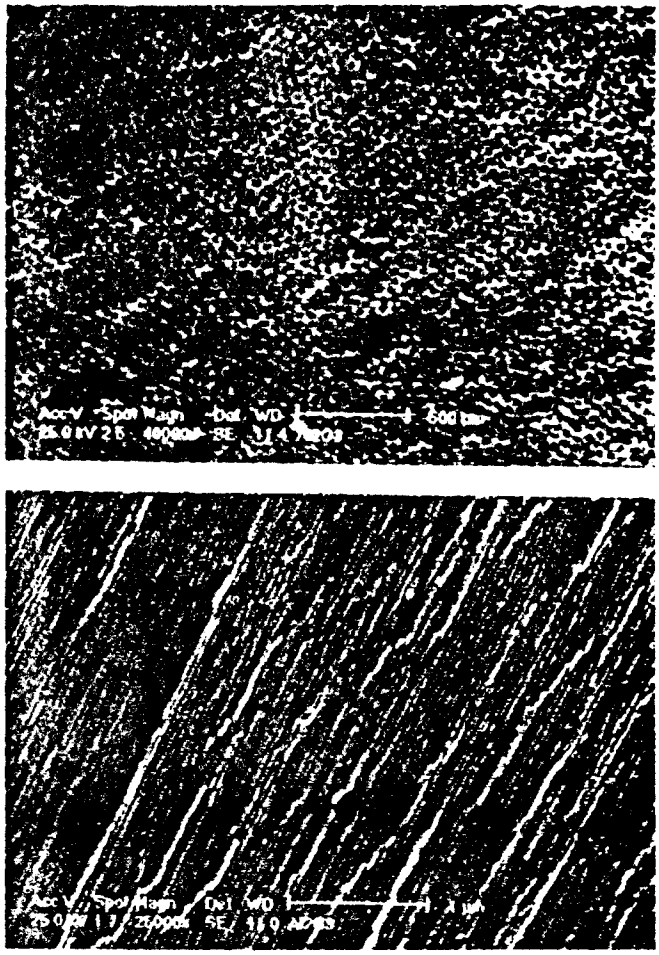

Figure 4. SEM Image of the surface of the electrochemically produced Al_2O_3. a) Low magnification picture of the cross section band structure b) high magnification picture of the pores.

MoS_2 Nanotubes

Yacamán and coworkers reported that MoS_2 nanotube structures can be produced by a very intense electron beam irradiation[36]. Using another method, Remskar et al. have grown MoS_2 giant, micron sized tubes called "microtubes".[37] Recently, Zelenski and Dorhout have produced nanotubes of MoS_2 using a template.[38] Using a low-temperature method developed by Müller,[39] they produced MoS_2 from solution-phase precursors within the porous membrane of an electrochemically produced Al_2O_3. In a recent paper this method was used to produce MoS_2 nanotubes that were characterized using high-resolution electron microscopy (HRTEM) and electron diffraction. The properties of the MoS_2 nanotubes were also investigated by using computer simulations. Resulting structural predictions regarding the structural stability indicated that MoS_2 nanotubes are not stable below a minimum diameter.[40]

Nanotubes of MoS_2 were prepared using the template approach in which nanoporous alumina templates were

Mat Tech & Adv Perf Mat 59
2000 15.1:35-84

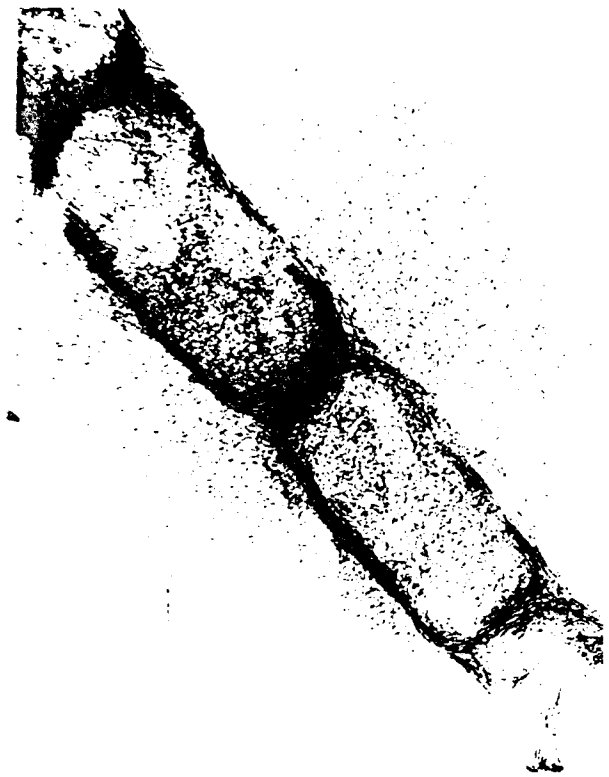

Figure 5. HRTEM image of a section of a MoS_2 tube

produced by anodization of aluminum. In order to obtain the MoS_2 nanotubes a solution of $(NH_4)_2MoS_4$ in dimethylformamide (DMF) was used as a solution-phase precursor. Small pieces of alumina template were immersed into the solution for a few seconds. Templates were dried at 70°C on a hot plate until the solvent evaporated. The samples were loaded into a quartz tube, which was put into a horizontal furnace and treated with a mixture of 10% H_2/N_2 at 450°C. The MoS_2 nanotubes were then removed from the templates and characterized by HRTEM.

In Figures 4a and 4b two images of the Al_2O_3 template used to produce the MoS_2 nanotubes are shown. The figure shows low and high magnification SEM pictures of the surface and the cross section of the template. As can be observed in Figure 4a the surface has banded features in which pores 25nm in diameter exist in a regular distribution. In Figure 4b it is possible to observe that the pore length is about 25μm wide and 250μm long. The MoS_2 tubes were grown in the pores of the template. A high-resolution image of a typical nanotube is shown in Figure 5. It can be seen that the tube is long up to 260nm. However, longer tubes with lengths up to ~1000nm are also present. Higher magnification micrographs show that the (002) planes of the MoS_2 structure are at the border of the tubes with an average interplanar distance of about 6.25 Å and an interplanar distance of about 2.74 Å (100 plane). This value is larger than the 6.16 Å expected for crystalline MoS_2. It should also be noted that the (002) planes are not seen in the interior part of the tube indicating typical contrast for a tubular structure. The structure as determined by electron diffraction corresponds to a 2H-MoS_2 nanotube. The (002) reflection also shows an expansion to 6.22 Å of the lattice parameter as noted above.

It was noted that the tube is not continuous, but it is split in several segments, each one with a diameter from 15-30 nm and a length between 150-500 nm. Generally, the sections of the tube are ellipsoidal. However, Figure 5 shows that in some cases, the shape are distorted as in the last section of a long tube. Also the planes of the nanotube are bent. This fact is similar to the bending of carbon nanotubes previously reported.[41]

MoS_2 crystallizes in a hexagonal system in which the Mo cation is at the center of a trigonal prism formed by 6 S atoms (S^{2-}). These geometrical units are then assembled into a layered structure with successive S-Mo-S slabs. These slabs are held together by van der Waals forces. Figure 6 shows a model of a MoS_2 nanotube including two layers built with a CERIUS2 (Molecular Simulations Incorporated) molecular simulation program. Starting with MoS_2 in trigonal prismatic coordination, and searching for the minimum energy configurations, stable configurations for cylinders of different sizes were found. Analyzing the Mo-S distances in the tubes and reported

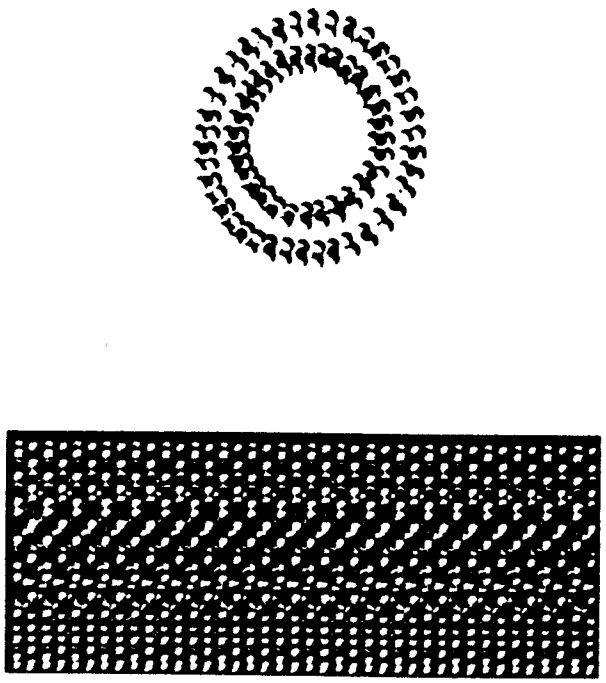

Figure 6. Simulation (CERIUS2) of a MoS_2 nanotube formed by two layers with lateral and top views of the tube.

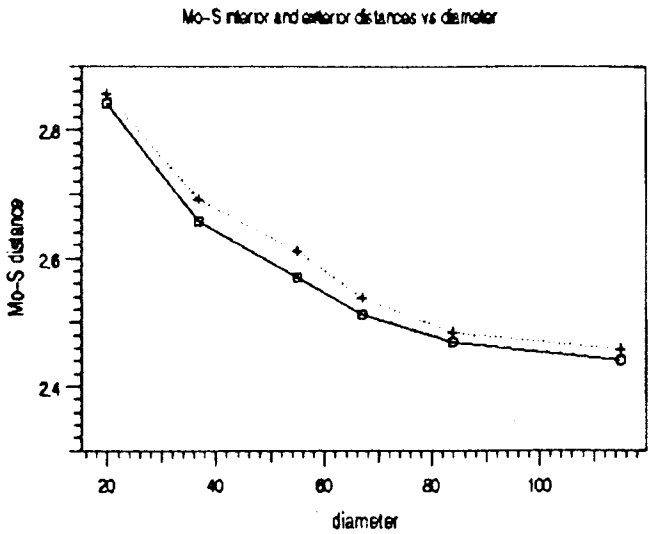

Figure 7. Interior and exterior distances as a function of tube diameter.

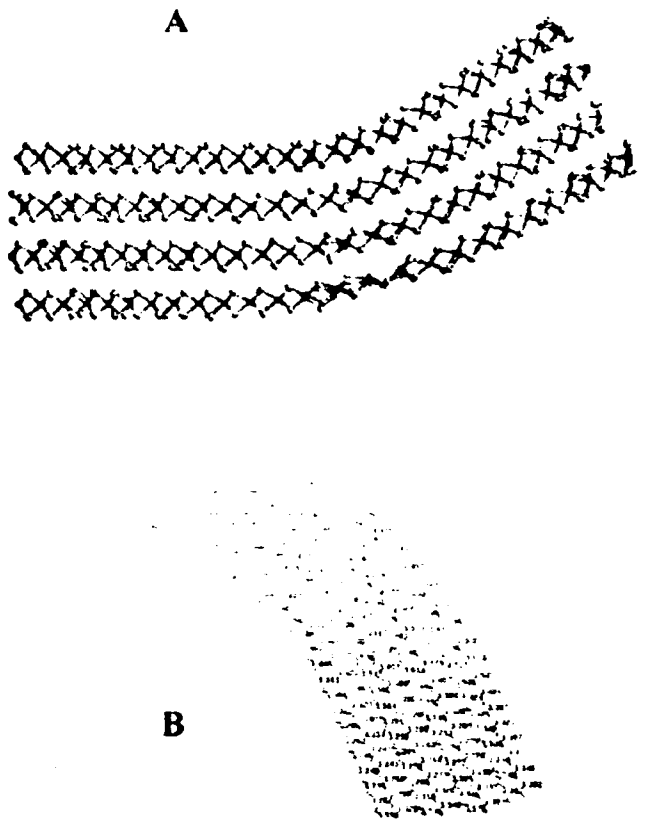

Figure 8. a) Model of a bent sheet (30 degrees) of MoS2 (with four layers). b) Atoms position measurements for a similar sheet.

two groups of measurements: one group contains the interior Mo-S distances (Mo-S (int)) and the other the exterior Mo-S distances (Mo-S (ext)). The mean distance for the Mo-S interior bonds is 2.65 Å and the mean distance for the exterior bonds is 2.75 Å. The calculation strongly implies that MoS_2 nanotubes of this diameter are not stable because bending to form a tube of this diameter requires stretching the Mo-S bonds well beyond their normal length of 2.41 Å. Using the this approach the mean distance for six tubes of various diameters between 20 and 120 Å was calculated and the results are plotted in Figure 7e. We note that the mean value of both the interior and exterior Mo-S bonds approach the single crystal value of 2.41Å. This implies that below a value of approximately 120 Å the tubes may be highly unstable because of bond strain. The MoS_2 nanotubes produced in this report are larger than this value.

The experimental MoS_2 nanotubes presented bent zones ("or knees"). Yacaman and coworkers have reported that in the case of MoS_2 crystals, a bending effect is often observed on the edges of the surface[18]. Therefore, it is important to understand the bending of MoS_2 sheets. Figures 8a and b present the model of a bent sheet of MoS_2 consisting of four layers of MoS_2. By examining the values of the S-S and Mo-Mo distances, a very large distortion appears clearly in the bent zone. Indeed, in comparison with the distances in the straight sections of the sheet, an increase of 20% in the distance between neighboring atoms is observed. This further emphasizes the instability of bent layers when the radius of curvature is small.

Discussion

Synthetic nanotubes, lubricants and catalysts all show similar bending phenomenon. Yacaman and coworkers reported that even in the case of MoS_2 crystals, a bending effect is often observed at the edges of the crystal surface. This study shows that while large MoS_2 nanotubes can be synthesized their minimum size is limited by the strain induced by stretched Mo-S bonds that are required to close tubes with diameters less than approximately 10nm. Tenne et al. reported the synthesis of WS_2 nanotubes with diameters in the range of 10nm[14]. However, a close examination of the micrographs reported in their paper reveals that the "nanotubes" become broken and discontinuous, as the diameter becomes smaller in agreement with this study. This is in contrast to nanotubes of carbon which exist down to very small diameters due to the change in carbon bonding which is inherent in fullerene based materials. Layered materials such as MoS_2 and WS_2 cannot close into small nanotubes unless a change in Mo-S bonding occurs. A change from six coordinate to a lower metal coordination might result in smaller diameter nanotubes. This phenomenon has not been reported at this writing, but is conceivable based on the known chemistry of Mo and S.

A further point of discussion is why the nanotubes made by the template method are not infinitely long but break into sections giving the shape of a "Spanish chorizo".

Calculations indicate that in principle there is no structural reason or energetic reason for the nanotube not to grow infinitely. The total energy of the nanotube will always be minimized by the distortion from the edge to the center described in the previous section. On the other hand HRTEM images clearly show that two sections of the tube are in contact but each one is preserving its corresponding layers. Therefore it is very likely that the sections are produced as a result of the growth kinetics. Zelenski and Dourhot have proposed that the morphologies observed are the result of the shape of the thiomolybdate precursor remaining within the confining template after the solvent has evaporated[39]. They based their conclusion on the evidence of studies of the evaporation of solvents on a wet table surface, which indicate the liquid remaining might form complex two-dimensional pattern. In that case the shape of the nanotubes will reflect the shape of the thiomolybdate precursor.

Acknowledgements: We would like to acknowledge the support of the National Science Foundation, the Robert A. Welch Foundation and CONACyT-Mexico for support of this project.

References:

1. S. Ijima. Nature. 354, 56 (1991).
2. M. Endo, S. Ijima and M. Dresselhaus, "Carbon Nanotubes" Pergamon Press, New York (1996).
3. S. Ijima, C. Brabec, A. Martí and J. Bernholc, J. Chem. Phys. 104, 7089(1996).
4. B. I. Yakobson, C. J. Brabeck and J. Bernholc. Phys. Rev. Lett. 76, 2511(1996).
5. O. Lourie, D. Cox and H.D. Wagner. Phys. Rev. Lett. 81, 1638(1988).
6. H. Dai, N. Franklin and J. Han. Appl. Phys. Letters 73, 1508(1998).
7. O. Weiser and S. Landa, Sulfide Catalysts: Their Properties and Applications (Oxford: Pergamon, 1973).
8. M. Daage and R.R. Chianelli, J. Catal. 149, 414 (1994).
9. P.D. Fleishauer, Thin Solid Films 154, 309 (1987).
10. M.S. Whittingham, Science 192, 1126 (1976).
11. H. Tributsch, Faraday Discuss. Chem. Soc. 70, 371 (1981).
12. M.S. Whittingham and A.J. Jacobson, ed. Intercalation Chemistry. (Academic Press: New York, 1982).
13. J.A. Wilson and A.D. Yoffe, Adv. Phys. 18, 193 (1969).
14. R. Tenne, L. Margulis, M. Genut, and G. Hodes, Nature 360 444 (1992).
15. Y. Feldman, E. Wasserman, D. Srolovitz, and R. Tenne, Science 267, 218 (1995).
16. E. Lu, P.D. Persans, A.F. Ruppert, and R.R. Chianelli, Mat. Res. Soc. Symp. Proc. 164 (1990) 153.
17. P.D. Persans, E. Lu, J. Haus, G. Wagoner, and A.F. Ruppert, Mat. Res. Soc. Symp. Proc. 195, 591 (1990).
18. R.R. Chianelli, A.F. Ruppert, M.J. Yacaman, and A.V. Zavala, Catalysis Today 23 269-281 (1995).
19. C.B. Roxlo, H.W. Deckman, J. Dunsmuir, A.F. Ruppert, and R.R. Chianelli, Mat. Res. Soc. Symp. Proc. 82, (1987).
20. W.M.R. Divigalpitiya, R.F. Frindt, and S.R. Morrison, Science 246, 369 (1989).
21. W.M.R. Divigalpitiya, S.R. Morrison, and R.F. Frindt, Thin Solid Films 186, 177 (1990).
22. W.M.R. Divigalpitiya, R.F. Frindt, and S.R. Morrison, J. Mat. Res. 6, 1103 (1991).
23. J.P. Wilcoxon, G. Samara, and P. Newcomer, Mat. Res, Soc. Symp. Proc. 358 277 (1995).
24. J.P. Wilcoxon and G.A. Samara, Phys. Rev. B 51 (1995).
25. F. Parsapour and J. Wilcoxon, J. Chem. Phys. 104, 4978 (1996).
26. R.R. Chianelli, Int. Rev. Phys. Chem. 2, 127 (1982).
27. R.R. Chianelli, Catal. Rev. Sci. Eng. 26, 361 (1984).
28. R.R. Chianelli, A.F. Ruppert, S.K. Behal, B.H. Kear, A. Wold, and R. Kershaw, J. Catal. 92, 56 (1985).
29. Y. Feldman, E. Wasserman, D. Srolovitz, and R. Tenne, Science 267 (1995) 218.
30. R.R. Chianelli and M.B. Dines, Inorg. Chem 17, 2758 (1978).
31. D.M. Schleich, Solid State Ionics, 70, 407(1994).
32. R.R. Chianelli, E. Prestridge, T. Pecoraro, and J.P. DeNeufville, Science, 203, 1105 (1979).
33. M.S. Dresselhaus and G. Dresselhaus, Ann. Rev. Mat. Sci. 25, 487 (1995).
34. F.A. Trumbore and L.W. ter Haar, Chemistry of Materials, 1, 490 1989.
35. P.A.Salyer and L.W. ter Haar, ACS Symposium Series, Chapter 5, 67 (1996).
36. M. José-Yacamán, H. López, P. Santiago, D. Galván, I. J. Garzón and A. Reyes, Appl. Phys. Lett., 69, 351(1996).
37. M. Remskar, Z. Skaraba, F. ClÈton, R. SanjinÈs and F. Levy. Appl. Phys. Lett. 69, 351(1996).
38. C. Zelenski and P. Dorhout. J. Am. Chem. Soc., 120, 734(1998).
39. T. Prasad, E. Diemann and A. Muller. J. of Inorg. Nucl. Chem., 35, 1895(1973).
40. P. Santiago, D. Mendoza, A. Espinosa, J. A. Ascencio, M. José Yacamán, R. R. Chianelli and G. Berhault. J. Mat. Res., submitted (1999).
41. B. I. Yakobson and R. Smalley, American Scientist, 85, 324(1997).
42. R. R. Chianelli, M. Daage and M.J. Ledoux. Advances in Catalysis 40, 177(1994).
43. C. Redon. F. Bouchard-Wgart, F. Rondelez. Phys. Rev. Lett. 66, 715, (1991).
44. M. Elbrum and S. G. Lipson. Phys. Rev. Lett. 72, 3562, (1994).

Metal Coatings - Effects Of Deuterium Irradiation On Copper Deposited Aluminum 6061 Substrates

T. Battal, O.T. Inal
Materials and Metallurgical Engineering Department, New Mexico Tech, Socorro, New Mexico 87801
& K.L.Kurz, R.A. Causey,
Sandia National Laboratories, Advanced Materials Research Department, Livermore, California, 94550

There are several applications for metals where hydrogen isotope implantation may be a factor. One example is the inside of a fusion reactor. While most areas inside

Address for Correspondence : O.T.Inal, New Mexico Institute of Mining & Technology, Socorro, MN, USA. Tel : +1 505 835 5519, Fax : +1 505 835 5626, Email: inal@nmt.edu